



Comparative analysis of ZnO-catalyzed photo-oxidation of *p*-chlorophenols

Umar Ibrahim Gaya

Department of Pure and Industrial Chemistry, Bayero University Kano, 3011, Kano State, Nigeria

*Corresponding author at: Department of Pure and Industrial Chemistry, Bayero University Kano, 3011, Kano State, Nigeria. Tel.: +234.803.9169418; fax: +234.64.665904. E-mail address: umarqaya2000@yahoo.com (U.I. Gaya).

ARTICLE INFORMATION

Received: 09 December 2010
Received in revised form: 07 February 2011
Accepted: 03 March 2011
Online: 30 June 2011

KEYWORDS

Oxidation
Mechanism
Chlorophenol
ZnO
Photodegradation
Intermediates

ABSTRACT

The present study compares for the first time the photocatalytic oxidation of three *p*-chlorophenols (4-chlorophenol, 2,4-dichlorophenol and 2,4,6-trichlorophenol) in irradiated ZnO suspensions. The effect of operating parameters such as catalyst and concentration doses on the decomposition rate of these *p*-chlorinated compounds has been studied and optimized. The optimal feed concentration for each of the chlorinated phenolic compounds is 50 mg/L whereas the ZnO doses decreased as the number of chlorine substituent is increased. Kinetic profiles on the decomposition of chlorophenols over ZnO agreed with the pseudo-zeroth order rate scheme with rate constants following the order 2,4,6-trichlorophenol > 2,4-dichlorophenol > 4-chlorophenol. The validity of the pseudo zero order model could be linked to the initial doses of the chlorophenols used vis-à-vis the catalyst. The study revealed stable intermediates of photocatalytic chlorophenol transformation by high performance liquid chromatography (HPLC) and gas chromatography-mass spectrometry (GC-MS) technique. A combined mechanism is given to account for the photocatalytic destruction of the chlorophenols.

1. Introduction

Photocatalytic reactions of organic substances and their mechanisms have been the subject of interest due to their application in both environmental and industrial development [1]. Many photoactive materials have been utilized to derive a high number of processes having varied applications [2-4]. Among these applications photo-oxidation stands at the forefront of contemporary research owing to its cost-effectiveness and environmentally benign nature [5-7]. When water is used as medium for the photo-oxidation of organic compounds, their complete mineralization prevails owing to the presence of potent oxidizing species such as hydroxyl radical [8,9]. These lines account for the applicability of photo-oxidation to the decontamination of pollutants. Photocatalytic oxidation technology has attracted myriad reports dealing with fundamentals, functional preparations and integration. A number of active reports on conspicuous topics emerged from different research groups [10-12]. The mainstay of a basic photocatalytic process is the photocatalyst. TiO₂ is regarded as a performance yardstick due to its photochemical stability, photoactivity and inertness. However, owing to its high excitation energy only a small fraction of solar spectrum is absorbed. Subsequently, it became crucial to improve the methods of catalyst utilization, devise novel photocatalyst preparations or even alternative photocatalysts. The author has been involved in the synthesis of catalysts and their applications [13,14]. In this report ZnO-driven photo-oxidative transformation of *p*-chlorophenols is presented. Our major aim is to compare for the first time the photocatalytic transformation of 4-chlorophenol (4CP), 2,4-dichlorophenol (24DCP) and 2,4,6-trichlorophenol (246TCP) with respect to operating doses, kinetics and oxidative products. The probable

general mechanism of photoproduct formation will be proposed and discussed.

2. Experimental

2.1. Chemicals

4-Chlorophenol was obtained from Fluka Chimie, 2,4-dichlorophenol and 2,4,6-trichlorophenol were supplied by Merck-Schuchard. Stock solutions were prepared using deionized distilled water and used fresh. The difficulty arising from the lower solubility of 24DCP and 246TCP was overcome by stirring overnight. HPLC grade solvents were used for HPLC and GC-MS analysis. Chemical standards were of high purity (≥99 %). All photoexperiments were carried out in an immersion well photoreactor maintained at 299 K. The features of the photoreactor were previously described in detail [13]. Irradiation was provided by 6W UV lamp having maximum intensity at 365 nm. The lamp was equilibrated for 25 min before use.

2.2. Photocatalyst characterization

ZnO (99 % purity) was obtained from Merck. The particle size of this material was measured on NANOPHOX at 298 K. This facility can measure sizes within 1 nm to 10 μm range. In a typical measurement, ZnO (0.1 %) suspension in water was diluted (x 4) at natural pH and sonicated (4 min) to disperse agglomerates. Aliquot (ca. 3 mL) was transferred to 10 x 10 sq. mm borosilicate cuvette for analysis. Replicate measurements were carried and average result was acquired from the NANOPHOX console.

In order to determine the surface area of ZnO which would be in contact with the aqueous environment during photocatalytic experiments, nitrogen adsorption was measured at 77.13 K by static volumetric gas method using Thermo Finnigan Sorptomatic 1990 Series analyzer. Surface area analysis was based on the BET principle introduced by Brunauer *et al.* [15].

Perkin Elmer Lambda 35 UV-Vis-NIR was used for band gap determination at room temperature. Sample holder was cleaned thoroughly, packed with ZnO and covered with quartz. The reflectance of these orderly-packed ZnO particles against non-absorbing standard was measured.

2.3. Procedure

A liter of solution comprising known amount of chlorophenol and ZnO photocatalyst was added to the photoreactor. Each reactivity solution was stirred for 5 min at 195 rpm to arrive at negligible mass gradient. Air was bubbled at the rate of 2 L/min. 20 mL of test samples were taken at predetermined time intervals (between 0 and 300 min) and passed through μm filter paper. The reaction progress was monitored by measuring the concentration of 10 mL sample on Shimadzu model UV-1650 PC UV-Vis spectrophotometer. Shimadzu model UV-1650 PC UV-Vis spectrophotometer was used to measure the concentration of chlorophenol in experimental samples. The maximum absorption wavelength of each chlorophenol was determined by scanning low concentration chlorophenol standard within 200 to 800 nm. Several standards were prepared for each chlorophenol usually in the range of 0 to 40 mg/L and calibration curves were drawn to the maximum correlation coefficient possible. The wavelengths of maximum absorption and the correlation coefficients of calibration graphs drawn for each chlorophenol are shown in Table 1.

Table 1. Wavelength maxima used in chlorophenol detection

Chlorophenol	Wavelength maximum (nm)	Correlation Coefficient (r^2)
4CP	225	0.9975
24DCP	284	0.9999
246TCP	294	0.9991

This facilitated direct interpolation of the concentration of chlorophenol in the unknown samples. The percentage of initial chlorophenol decomposed during photoreaction was calculated by Equation 1. In certain cases the percentage of chlorophenol removed was computed by dividing values obtained from Equation 1 by the irradiation time taken.

$$\text{Ph(Cl)}_x\text{OH} (\%) = \left(\frac{C_o - C_t}{C_o} \right) \times 100 \quad (1)$$

where C_o and C_t (mg/L) represent the initial concentration of 4CP, 24DCP or 246TCP at irradiation time $t = 0$ min and at $t = t$ min.

The transformation of chlorophenols was also monitored by using Waters HPLC installed with absorbance detector. Ascentis-C₁₈ column was utilized for the HPLC. The HPLC was adequately equilibrated before use. Mobile phase was continuously outgassed by Helium. The mobile phase delivery was optimized at 1 mL/min. Some operational parameters used for the reverse phase HPLC analysis of the chlorophenols are listed in Table 2.

HPLC was complemented by Shimadzu's GCMS-QP5050A for structural elucidation of photoproducts. Photoproducts were extracted by liquid-liquid method using diethyl ether, and concentrated to a few ml under nitrogen current. BPX-5 capillary column was used for GC separation. Carrier gas was helium. The capillary column was maintained at 70 °C for 2 min

followed by temperature increase at the rate of 10 °C/min up to 310 °C. The injector and detector temperatures were 250 °C and 320 °C respectively. Analytical data on degradation species were interpreted by National Institute of Standards and Technology (NIST) library.

Table 2. Selected parameters used in HPLC elution chromatography

Chlorophenol	Mobile phase (v:v)	Detection wavelength	Run time
4CP	CH ₃ OH:H ₂ O (60:40)	280 nm	30 min
24DCP	CH ₃ CN:CH ₃ COOH:H ₂ O (69:1:30)	284 nm	20 min
246TCP	CH ₃ OH:CH ₃ COOH:H ₂ O (70:1:29)	280 nm	30 min

3. Results and discussion

3.1. Properties of the ZnO catalyst

Band gap is very crucial to know the wavelength of light that can excite the semiconductor photocatalyst [16]. To determine band gap, ZnO specimen was measured in the reflectance mode of Perkin Elmer Lambda 35 UV/Vis/NIR. The optical band gap (E_g) was estimated from the intercept of the extrapolated tangent of the plot of logarithmic remission function ($\ln\alpha/S$) against photon energy ($h\nu$) (Figure 1), where α and S represent absorption and scattering coefficient, respectively. The band gap energy extrapolated from the plot was 3.36 eV. The ratio α/S was calculated from the experimentally measured reflectance (R) by Kubelka-Munk equation [16]:

$$\frac{\alpha}{S} = \frac{(1-R)^2}{2R} \quad (2)$$

α/S is referred to as Kubelka-Munk or remission function and is interchangeably used with $F(R)$. α varies with the light energy absorbed according to Tauc's equation [17,18]:

$$\alpha h\nu \propto (h\nu - E_g)^n$$

or

$$(\alpha h\nu)^{1/n} \propto (h\nu - E_g) \quad (3)$$

where n is a constant accounting for the type of optical transition. Assuming direct optical transition and remarkably effective absorption then $n = 1/2$ and $\alpha = F(R)$, respectively. Subsequently, the Tauc band gap can be obtained as intercept of the plot of $(\alpha h\nu)^2$ or $(F(R)h\nu)^2$ against $h\nu$. The band gap of ZnO was confirmed via the latter to be 3.36 (Figure 1, inset).

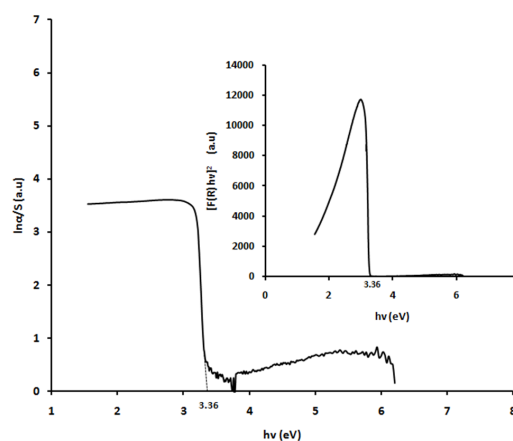


Figure 1. Kubelka-Munk spectral function of ZnO photocatalyst versus excitation energy. The inset is a Tauc plot depicting the variation of $(F(R)h\nu)^2$ against light photons absorbed.

Particle size has marked influence on the activity of semiconductor photocatalyst [19]. The particle sizes of the photocatalyst were computed by the method of Second Cumulant. Figure 2 shows the distribution of particle size in the ZnO powder against their cumulative distribution. From the figure, the highest cumulative distribution was obtained at 493 nm.

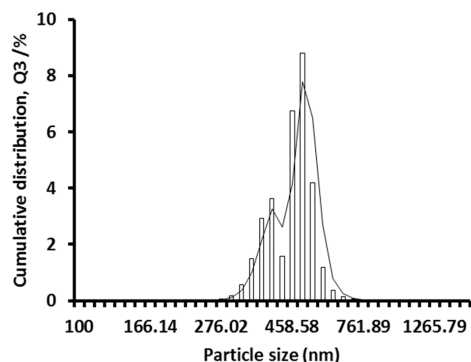


Figure 2. Particle sizes of the ZnO (Merck) used in the study of chlorophenols plotted against cumulative distribution.

The surface area of ZnO was recorded on Sorptomatic 1990 Series analyzer following Brunauer-Emmett-Teller (BET) gas adsorption. The surface area evaluated by static BET method was $3.28 \text{ m}^2\text{g}^{-1}$. We have previously shown that this low surface area is responsible for the activity of the Merck ZnO [20]. Previously, a lower surface area ($1.56 \text{ m}^2/\text{g}$) was reported for Merck ZnO powder by Marto *et al.* [21].

3.2. Effect of catalyst and substrate concentration

Generally in environmental photocatalysis, effective decontamination is only achieved at optimum doses of the photocatalyst and the substrate. Therefore the effect of concentration of each of the three chlorophenols was studied by varying chlorophenol concentration between 30 mg/L and 100 mg/L at a fixed ZnO load (1 g) for a period of 300 min. Figure 3 displays the relative effect of the concentration of 4CP, 24DCP and 246TCP on photoremoval rate measured as % removed per unit irradiation time. A preliminary investigation with low level (10 mg/L) 4CP and 24DCP revealed high removal rate and this maintained a level performance with 30 mg/L initial concentration. At 50 mg/L the photoremoval rate began to fall probably as a result of the inadequacy of catalyst sites. This effect became more pronounced as the concentration of the phenolic substrates is increased. Similarly, the photocatalytic removal rate of 246TCP diminished between 50 mg/L and 100 mg/L initial chlorophenol concentration. As a result, 50 mg/L of each of the chlorophenols was used as initial concentration throughout this study.

The effect of catalyst concentration was studied at the 50 mg/L chlorophenol concentration. Figure 4 shows the influence of the catalyst concentration on the photo-oxidative removal of 4CP, vis-à-vis 24DCP and 246TCP. It would be observed that there is no removal of any chlorophenol in the absence of the photocatalyst. This affirms the photocatalytic nature of the process and rules out the influence of photolysis. For each of the chlorophenols there has been increase in photocatalytic removal as catalyst concentration is increased due to increasing availability of active sites. It would be observed that the photocatalytic performance declined as the catalyst amount reaches 2.00 g/L, 1.50 g/L and 0.75 g/L for 4CP, 24DCP and 246TCP, respectively. The decrease in degradation rate would be attributed to light scattering and reduced light penetration.

Hence, these catalyst concentrations were considered optimum for the study.

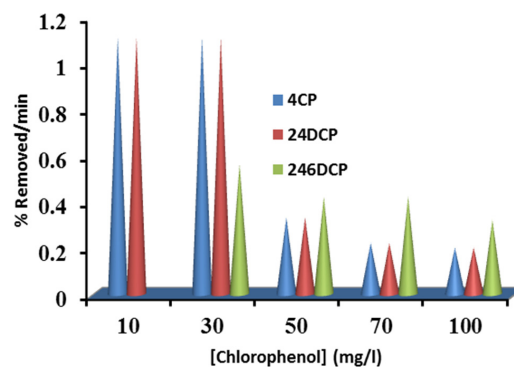


Figure 3. Influence of concentration on photo-oxidative removal of chlorophenols from water. Initial ZnO concentration = 1 g/L; Initial chlorophenol concentration = 30-100 mg/L; pH = 7.20-7.99 (normal solution pH).

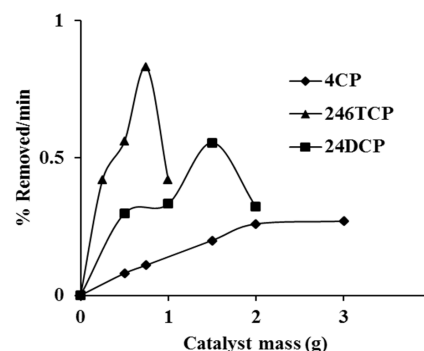


Figure 4. Effect of catalyst dose on chlorophenol concentration removal from aqueous solution. Initial 246TCP concentration = 50 mg/L; pH = normal; 6.45-7.50.

3.3. Photocatalytic kinetic model

The photocatalytic oxidation of all the three *p*-chlorinated compounds on ZnO surface agreed with the pseudo zero-order rate model expressed by Equation 4.

$$C_t = C_0 - kt \quad (4)$$

where C_0 and C_t are as previously defined, k is the pseudo zero order rate constant and t is irradiation time. The pseudo zero order rate constant for the oxidative removal of each chlorophenol is shown in Table 3. The validity of pseudo zero order model could be linked to the fact that the initial concentration of substrates was high enough to occupy wholly the active sites. This information is captured in Figure 4 which shows no availability of active sites above 50 mg/L initial ZnO concentration. The consistency of the degradation of the chlorophenols with pseudo zero order was measured by correlation as R^2 . Perhaps the reduction in agreement with zero order in 24DCP and 246TCP is due to the formation of more recalcitrant intermediates. In this connection, we have recently highlighted on the nature of the decomposition and the possible reasons for diminishing kinetic consistency [20,22].

Table 3. Rate constants for the pseudo zero order disappearance of chlorophenol in ZnO suspensions.

Chlorophenol	ZnO (g/L)	k (mg/L min)	r^2
4CP	2.00	0.25	0.9978
24DCP	1.50	0.38	0.9864
246TCP	0.75	0.42	0.9637

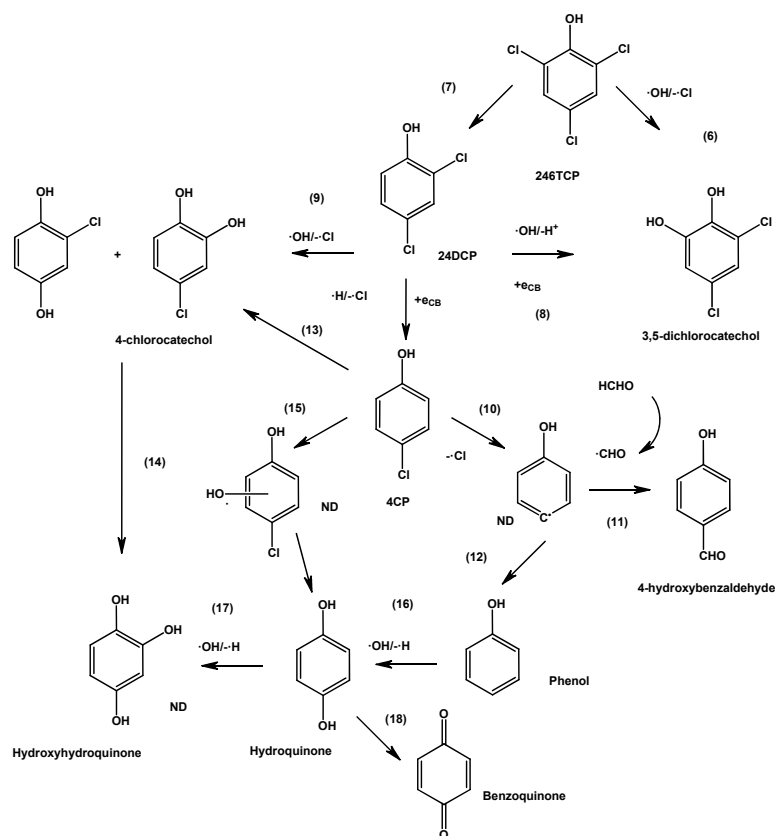
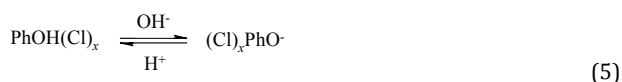


Figure 5. Intermediates of photocatalytic transformation of 4CP, 24DCP and 246TCP, and tentative mechanism of their formation. ND indicates intermediates not determined but traceable to other literature.

3.4. Effect of solution pH

In order to investigate the influence of solution acidity on photocatalytic degradation rate the effect of pH was studied. To avoid common ion effect, non Cl⁻ containing pH adjustment chemical was used. The degradation of all chlorophenols was found favorable only in the slightly alkaline solution pH. 4CP showed its highest photocatalytic degradation at pH = 9 where as 24DCP and 246TCP were more degradable at pH = 7. The photoprocess was inhibited further below pH = 7 with all of the p-chlorophenols. For example, 4CP did not degrade at pH = 4. This is probably as a result of the stability of the molecular form of these chlorophenols as shown by Equation 5. The reverse effect was observed at strongly alkaline solution pH.



3.5. Reaction intermediates and mechanism

The structural elucidation of photoproducts during the course of mineralization of chlorophenols was performed by GC-MS and HPLC methods. We have recently disclosed the intermediates of the photocatalytic decomposition of 4CP, 24DCP and 246TCP [13,20,22]. Interestingly, 24DCP and 246TCP both produced 3,5-dichlorocatechol and 4CP (which is a lower chlorophenol). Moreover, all the chlorophenols under study yielded phenol en route to their decomposition. Based on this fact we propose a general mechanism to account for the formation of these intermediates. Figure 5 shows the detected intermediates and depicts a tentative mechanism to account for their formation. The detected intermediates are mostly

hydroxylated, dehydroxylated or dechlorinated products falling into higher or lower molecular weight phenolic class. The formation of these intermediates can be attributed to the oxidative action of hydroxyl radical [23,24] which may take place via oxidative cleavage and/or hydroxylation. It would be seen from the figure that 246TCP yielded 3,5-dichlorocatechol by simultaneous dechlorination-hydroxylation (Equation 6). By the same process (Equation 9) 2-chlorohydroquinone or 4-chlorocatechol could be formed from 24DCP. Similarly, the hydroxylation of 4CP will yield the same products (Equation 13). Perhaps phenol is the last phenolic formed in the transformation mechanism. Several literature [25,26] have shown that hydroquinones and subsequently benzoquinones are formed finally which would decompose to form aliphatics and then carbon dioxide and water. We have also detected hydroquinone and benzoquinone during 4CP and 24DCP degradation, respectively.

3.6. Effect of activating substituents

Naturally, the activating substituents (-OH and -Cl) on the phenolic ring groups would be expected to cause increase the reactivity of the phenolic rings. Our results accordingly (Table 3) show lesser resistance of the chlorophenolic substrates to photo-degradation on ZnO as the number of ring-Cl is increased. From this point of view therefore, we would expect 3,5-dichlorocatechol to be more photoreactive than the 24DCP from which it is formed. Each of the chlorophenols has been found to yield at least a product with -OH in the ortho- or para-orientation relative to the phenolic-OH. Thus, 3,5-dichlorocatechol was obtained on the photodegradation of 24DCP and 4-chlorocatechol was obtained from the oxidation of 4CP.

4. Conclusion

A comparative analysis of the photocatalytic oxidation of 4CP, 24DCP and 246TCP with ZnO has been made for the first time. The photocatalytic process is consistent only with pseudo zero order integrated rate law. Several common hydroxylation products have been determined in the ZnO photo-assisted oxidation of 4CP, 24DCP and 246TCP and a general mechanism has been proposed. The study revealed the influence of phenolic-OH over phenolic-Cl as an ortho-para directing group with each of the chlorophenols which supports the common knowledge that -OH is ab initio stronger ortho-para directing group than -Cl. As the number of ring-Cl of *p*-chlorophenol is increased the ease of oxidative transformation or degradation is favored which confirms the activating effect of the substituent groups on the phenolic ring. Accordingly, the amount of catalyst required reduces with increase in the number ring-Cl bonds.

Acknowledgement

The author is grateful to Khairul Basyar Baharuddin and Huda Abdullah Universiti Putra Malaysia, for their assistance with diffuse reflectance measurement.

References

- [1]. Yin, D.; Hu, S.; Jin, H.; Yu, L. *Chemosphere* **2003**, *52*, 67-73.
- [2]. Ichihashi, Y.; Matsumura, Y. *J. Catal.* **2001**, *202*, 427-429.
- [3]. Sehlotho, N.; Nyokong, T. *J. Mol. Catal. A: Chem.* **2004**, *219*, 201-207.
- [4]. Amadelli, R.; Bregola, M.; Polo, E.; Carassiti, V.; Maldotti, A. *J. Chem. Soc. Chem. Commun.* **1992**, 1355-1357.
- [5]. Augugliaro, V.; Kisch, H.; Loddo, V.; López-Muñoz, M. J.; Márquez-Álvarez, C.; Palmisano, G.; Palmisano, L.; Parrino, F.; Yurdakal, S. *Appl. Catal. A* **2008**, *349*, 182-188.
- [6]. Singh, H. K.; Saquib, M.; Haque, M. M.; Muneer, M.; Bahnemann, D. W. *J. Mol. Catal. A: Chem.* **2007**, *264*, 66-72.
- [7]. Li, S.; Ma, Z.; Zhang, J.; Wu, Y.; Gong, Y. *Catal. Today* **2008**, *139*, 109-112.
- [8]. Anpo, M.; Kamat, P. V. (Eds.). *Environmentally benign photocatalysts. Application of titanium oxide-based materials series: Nanostructure science and technology*. 1st edition, Springer, 2010.
- [9]. Alfano, O. M.; Cabrera, M. I.; Cassano, A. E. *J. Catal.* **1997**, *172*, 370-379.
- [10]. Fujishima, A.; Rao, T. N.; Tryk, D. A. *J. Photochem. Photobiol. C* **2000**, *1*, 1-21.
- [11]. Turchi, C. S.; Ollis, D. F. *J. Catal.* **1990**, *122*, 178-192.
- [12]. Minero, C.; Aliberti, C.; Pelizzetti, E.; Terzian, R.; Serpone, N. *Langmuir* **1991**, *7*, 928-936.
- [13]. Gaya, U. I.; Abdullah, A. H.; Zainal, Z.; Hussein, M. Z. *J. Hazard. Mater.* **2009**, *168*, 57-63.
- [14]. Abdullah, A. H.; Giat, L. E.; Gaya, U. I. *Surface and physicochemical properties of precipitation derived zinc oxide and its degradation to methyl orange, 12th Asian Chemical Congress (12ACC)*. Kuala Lumpur, Malaysia. August, 2007.
- [15]. Brunauer, S.; Emmett, P. H.; Teller, E. *J. Am. Chem. Soc.* **1938**, *60*, 309-319.
- [16]. Trikalitis, P. N.; Rangan, K. K.; Bakas, T.; Kanatzidis, M. G. *Nature* **2001**, *410*, 671-674.
- [17]. Tauc, J.; Menth, A. *J. Non-Cryst. Solids* **1972**, *8-10*, 569-585.
- [18]. Kako, T.; Kikugawa, N.; Ye, J. *Catal. Today* **2008**, *131*, 197-202.
- [19]. Dodd, A. C.; McKinley, A. J.; Saunders, M.; Tsuzuki, T. *J. Nanopart. Res.* **2006**, *8*, 43-51.
- [20]. Gaya, U. I.; Abdullah, A. H.; Hussein, M. Z.; Zainal, Z. *Desalination* **2010**, *263*, 172-182.
- [21]. Marto, J.; Marcos, P. S.; Trindade, T.; Labrincha, J. A. *J. Hazard. Mater.* **2009**, *168*, 57-63.
- [22]. Gaya, U. I.; Abdullah, A. H.; Zainal, Z.; Zobir, M. *Int. J. Chem.* **2010**, *2*, 180-193.
- [23]. Gaya, U. I.; Abdullah, A. H. *J. Photochem. Photobiol. C: Photochem. Rev.* **2008**, *9*, 1-12.
- [24]. Carp, O.; Huisman, C. L.; Reller, A. *Prog. Solid State Chem.* **2004**, *32*, 33-177.
- [25]. Theurich, J.; Lindner, M.; Bahnemann, D. W. *Langmuir* **1996**, *12*, 6368-6376.
- [26]. Li, X.; Cubbage, J. W.; Tetzlaff, T. A.; Jenks, W. S. *J. Org. Chem.* **1999**, *64*(23), 8509-8524.